

Decay Schemes of Sm^{145} and $\text{Pm}^{145}\dagger$ A. R. BROSI, B. H. KETELLE, H. C. THOMAS,* AND R. J. KERR†
Oak Ridge National Laboratory, Oak Ridge, Tennessee

(Received August 18, 1958)

The electron capture decay schemes of Sm^{145} and Pm^{145} have been investigated. The total disintegration energy of Sm^{145} was found to be 645 ± 15 kev by measurement of the inner bremsstrahlung energy end point. The fraction of electron captures to the 61-kev level that are K -electron captures was computed to be 0.83 ± 0.02 from conversion electron-x-ray coincidence counting rates. The same coincidence method gave 0.54 ± 0.02 as the K -electron capture fraction in Pm^{145} decay to the 67 kev level in Nd^{145} . From the experimental capture ratio the transition energy was computed to be 73 ± 10 kev. The lifetime of the 61-kev level in Pm^{145} was found to be 2.6×10^{-9} sec and that of the 67-kev level in Nd^{145} was found to be 3.3×10^{-8} sec. Conversion coefficients of the gamma rays emitted in Sm^{145} and Pm^{145} decay were measured. Energy level schemes which have spin and parity assignments consistent with the experimental measurements are proposed for both isotopes.

INTRODUCTION

RADIOACTIVE decay of Sm^{145} was first observed¹ in a mass spectrographic study of samarium activated in a reactor. This work indicated that the Sm^{145} half-life was greater than 72 days and that the Pm^{145} half-life was an order of magnitude different from that of the Sm^{145} parent. In a study of reactor-produced Sm^{145} , Butement² found the half-life to be 410 days. From the relative intensity of the K x-rays associated with the promethium daughter he calculated a half-life of 30 years for Pm^{145} . He reported no other radiations associated with either of these mass-145 isotopes.

Rutledge, Cork, and Burson³ found the conversion electrons of a 61.3-kev gamma ray associated with Sm^{145} . They reported a K/L conversion ratio for this gamma ray of unity. In work with samarium enriched in Sm^{144} , which had been bombarded for a year at an average neutron flux of 3×10^{13} neutrons/cm² sec, Parker and Martin⁴ found the Sm^{145} half-life to be about 1 year and the Pm^{145} half-life to be much longer. They also found low-energy gamma radiation (70 to 80 kev) associated with Pm^{145} decay.

In the present study the gamma radiation emitted by Pm^{145} was resolved into two components with energies of 67 kev and 72 kev. A new but very-low-intensity gamma ray was found to be emitted in Sm^{145} decay. Coincidence measurements were made using magnetic lens, scintillation counter, and proportional counter spectrometers for energy discrimination. From these data L/K electron capture ratios, branching ratios, and conversion coefficients were computed. In the case of Sm^{145} the energy end points of x-ray- and gamma-ray-coincident inner bremsstrahlung radiation

were determined. Half-lives for both Sm^{145} and Pm^{145} were remeasured.

Energy level diagrams with spin and parity assignments consistent with the experimental data are proposed for both isotopes.

PREPARATION OF SOURCES

Most of the work with Sm^{145} reported here was done with samarium enriched in Sm^{144} which was bombarded for one year at a neutron flux of 3×10^{13} neutrons/cm² sec. After the bombardment the samarium was separated from Pm^{145} and Pm^{146} which grew during the irradiation and from traces of other rare earths by elution from Dowex-50 ion exchange columns. Promethium-145 activity was obtained by letting the purified samarium stand for periods of months and then separating the daughter Pm^{145} from the parent Sm^{145} on an ion exchange column. This procedure gave Pm^{145} of high specific activity, which was suitable for use in beta-spectrometer sources. The specific activity of the Sm^{145} was not high enough to use in studies of the low-energy conversion electrons on a magnetic lens spectrometer. Sources of Sm^{145} for this purpose were prepared by bombarding samarium-free neodymium oxide with 45-Mev alphas on the Berkeley 60-inch cyclotron. After irradiation the samarium produced by an (α, n) reaction was separated on an ion-exchange column from the neodymium target and from rare earths produced by other nuclear reactions. Separation from other solids in the column elutriant was achieved by precipitating samarium as the fluoride and then converting to the perchlorate. The beta spectrometer sources were mounted on $30 \mu\text{g}/\text{cm}^2$ of gold supported by a $50\text{-}\mu\text{g}/\text{cm}^2$ plastic film. Not more than a few $\mu\text{g}/\text{cm}^2$ of solid material was associated with either the Sm^{145} or the Pm^{145} spectrometer source.

SAMARIUM¹⁴⁵ MEASUREMENTS

A Sm^{145} gamma-ray spectrum taken at low geometry with a scintillation spectrometer is shown in Fig. 1. This confirms the presence of the previously reported

† This paper is based upon work performed at Oak Ridge National Laboratory which is operated by Union Carbide Corporation for the U. S. Atomic Energy Commission.

* Present address: Texas Technological College, Lubbock, Texas.

† Instrument Division now of Applied Physics Division.

¹ Inghram, Hayden, and Hess, *Phys. Rev.* **71**, 643 (1947).

² F. D. S. Butement, *Nature*, **167**, 400 (1951).

³ Rutledge, Cork, and Burson, *Phys. Rev.* **86**, 775 (1952).

⁴ G. W. Parker and W. T. Martin, Oak Ridge National Laboratory Report ORNL-1432 (unpublished).

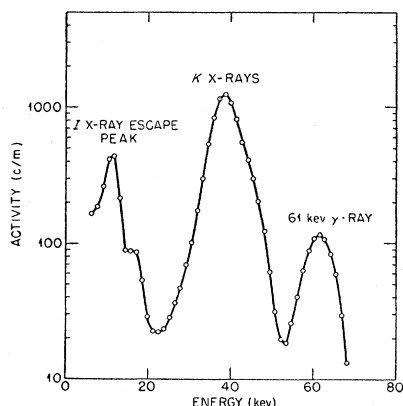


FIG. 1. Sm^{146} scintillation counter spectrum.

61-keV gamma ray. From this spectrum the ratio of K x-rays to 61-keV gamma rays was found to be 11.35. A spectrum taken with a much more intense source and 585 mg/cm² of tin to absorb the x-rays and 61-keV gamma ray is shown in Fig. 2. Repeated purification of the Sm^{146} did not change the relative intensities of the continuous spectrum and the 485-keV gamma ray peak. The half-lives of the x-rays, 61-keV gamma ray, 485-keV gamma ray, and the continuous inner bremsstrahlung spectrum were all found to be 340 ± 3 days. It was concluded that all of these radiations were associated with Sm^{146} decay and that the 61-keV gamma ray was 4.5×10^8 times as intense as the 485-keV gamma ray.

A 4π scintillation spectrometer curve taken with a detector assembly similar to that described earlier⁵ is shown in Fig. 3. A 0.9-mil aluminum absorber was placed between the Sm^{146} source and each of the NaI crystals to absorb Auger electrons and conversion electrons. The peaks in the spectrum labeled *A*, *B*, *C*, and *D* correspond, respectively, to absorption in the crystal of one K x-ray photon, two K x-ray photons,

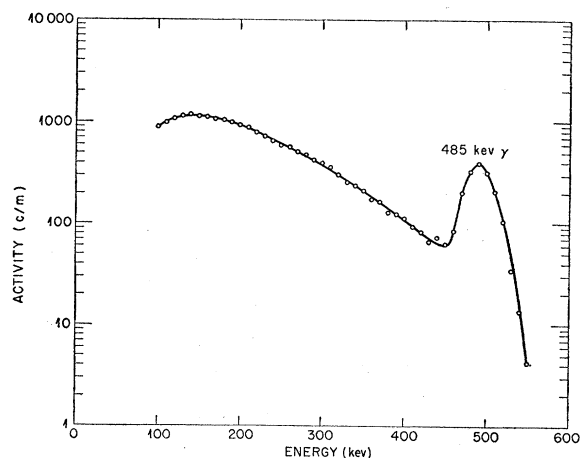


FIG. 2. Inner bremsstrahlung spectrum of Sm^{146} .

⁵ Ketelle, Thomas, and Brosi, Phys. Rev. 103, 190 (1956).

one 61-keV gamma ray, and absorption of a 61-keV gamma ray plus one K x-ray photon. If suitable corrections are made for the probability of detection of gamma rays and K -shell vacancies, the intensities of these peaks are proportional to the number of decay processes in which the particular radiations are emitted. Equations relating the areas of the peaks in the spectrum to the number of processes were given in an earlier publication.⁵ The K -conversion coefficient can be obtained from the ratio of the number of K captures followed by K conversion to the number of K captures followed by gamma emission. This gives α_K equal to 5.3 ± 0.2 for Sm^{146} . Values for the electron capture ratio ϵ can also be obtained from 4π data. However, in the case of Sm^{146} , since the peak corresponding to L capture followed by gamma emission has a low intensity and is not completely resolved from the K capture followed by K -conversion peak, the value of $\epsilon = 0.25 \pm 0.05$ obtained in this way is subject to large errors.

In work with Ce^{139} an estimate of β , the ratio of ground-state to excited-state K captures, was obtained by mounting the 4π source between thin films so that the conversion electrons as well as the x-rays and gamma rays were counted. The rate of K captures to the ground state with no other coincident radiation was equal to the counting rate in the K x-ray peak. In the case of Sm^{146} the 15-keV K -conversion electron energy is so low that not all of the electrons are counted. However, an estimate of β can be obtained from the counting rate in peak *A* of Fig. 3 relative to the counting rates in peaks *B* and *D*. If the counting rates in the peaks are corrected for the events which would have appeared in other peaks had all detection probabilities been unity, the remaining counting rate in peak *A* will be due to K captures followed by L conversion, L captures followed by K conversions, and K captures directly to the ground state. From the corrected

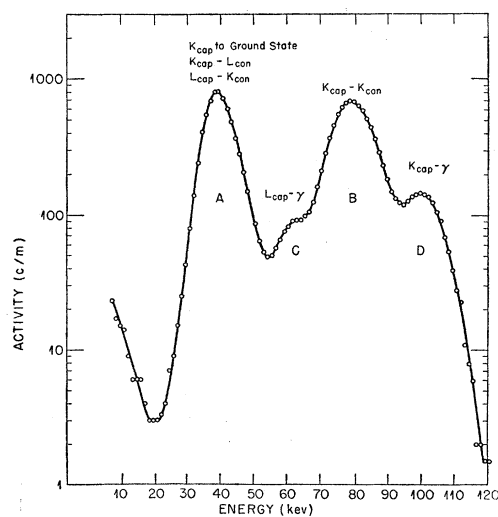


FIG. 3. 4π scintillation counter spectrum of Sm^{146} .

TABLE I. Sm^{145} experimental data.

Measurement	Method	Result
K/L conversion ratio 61-keV gamma	lens spec.	6.5 ± 0.4
L/M conversion ratio 61-keV gamma	lens spec.	5.1 ± 0.3
K Augers/ K conversions 61-keV gamma	lens spec.	0.24 ± 0.02
K -conversion coefficient 61-keV gamma	4π scin. spec.	5.3 ± 0.1
K captures to ground/ K captures to 61-keV level	4π scin. spec.	0.08 ± 0.02
K x-rays/61-keV gamma rays	scin. spec.	11.4 ± 0.4
485-keV gamma rays/61-keV gamma rays	scin. spec.	$(2.2 \pm 0.1) \times 10^{-4}$
K captures/61-keV K conversions	x-x and x- γ coinc.	1.24 ± 0.04
$(L+M+N)/K$ (captures to 61-keV level)	L -conversion electron-x-ray coinc.	0.20 ± 0.02
$(L+M+N)/K$ (captures to 485-keV level)	(485-keV γ and I.B.)-x-ray coinc.	0.6 ± 0.1
I.B. end point for capture to 61-keV level	61-keV γ -I.B. coinc.	525 ± 50 keV
Half-life of 61-keV level	delayed x- γ coinc.	$(2.6 \pm 0.2) \times 10^{-9}$ sec

counting rates in the peaks, the L/K capture ratio, and the K/L conversion ratio, the ratio of ground-state K captures to excited-state K captures has been computed to be 0.08 ± 0.02 .

The K/L conversion ratio was measured on a thin magnetic lens spectrometer. Because of the very low energy of the K line (15 keV) it was necessary to work with sources of very high specific activity and to use very thin counter windows. The value for the conversion ratio given in Table I was the limiting ratio found as the solids in the source were reduced and as the thickness of the counter window was reduced. Figure 4 shows the conversion-electron and Auger-electron spectrum of Sm^{145} .

The magnetic-lens spectrometer has also been used with a scintillation spectrometer to measure coincidences between K x-rays and conversion electrons. The L -conversion electron-x-ray coincidence rate, N_{xL} , the K -conversion electron-x-ray coincidence rate, N_{xK} , and the counting rates in the L - and K -conversion electron peaks, N_L and N_K , respectively, are related to the electron capture ratio ϵ as follows:

$$2 + \epsilon = \frac{N_L}{N_{xL}} \bigg/ \frac{N_K}{N_{xK}} \quad (1)$$

This equation is valid only when the x-ray counting efficiency is very low. At high x-ray counting efficiencies coincident K x-rays are absorbed in the detector and give pulses twice the size of a single x-ray pulse. Discrimination against these pulses eliminates some of the coincidences between K -conversion electrons and x-rays, but does not eliminate any of the coincidences between L -conversion electrons and x-rays. This leads to error in ϵ unless the equation is corrected by terms which are a function of the x-ray counting efficiency. A determination of ϵ using this equation gave 0.20 ± 0.02 , where the large statistical error results from the fact that ϵ is small in comparison with two.

The electron capture ratio can also be calculated from x-ray-x-ray and x-ray-gamma-ray coincidence measurements.⁶ The ratio of the coincidence counting

rates, N_{xx} and $N_{x\gamma}$, and the single counting rates in one channel, N_x and N_γ ,

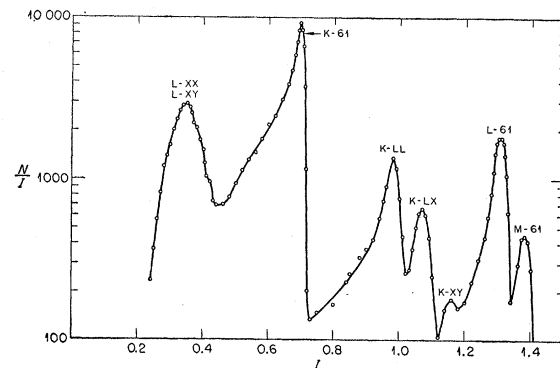
$$R_3 = \frac{N_{x\gamma}}{N_\gamma} \bigg/ \frac{N_{xx}}{N_x} \quad (2)$$

is related to the electron capture ratio as follows:

$$1 + \epsilon = \frac{1 + \beta}{2R_3 - 1} \left[\frac{1}{\alpha_K} + \frac{1 + R_1}{R_1} \right] \quad (3)$$

Here $1 + \epsilon$ is the ratio of total electron captures to the excited state to K -electron captures to the excited state, β is the ratio of ground-state to excited-state K -shell captures, α_K is the K -conversion coefficient and R_1 is the ratio of K conversions to $(L+M)$ conversions. Substituting values for these constants into the equation gives ϵ equal to 0.20 ± 0.05 . The rather large uncertainty in ϵ results from the fact that ϵ is small compared with one and from the errors in the other constants which appear in the equation. However, the value is consistent with the values found by the other methods reported above.

Delayed coincidences were measured between the K x-rays and the 61-keV gamma ray using a "fast-low" coincidence assembly⁷ with a resolving time of 8 μsec .


 FIG. 4. Magnetic lens spectrum of Sm^{145} .

⁷ R. E. Bell, in *Beta and Gamma Ray Spectroscopy*, edited by K. Siegbahn (Interscience Publishers, Inc., New York, 1955), p. 494.

⁶ C. H. Pruett and R. G. Wilkinson, *Phys. Rev.* **96**, 1340 (1954).

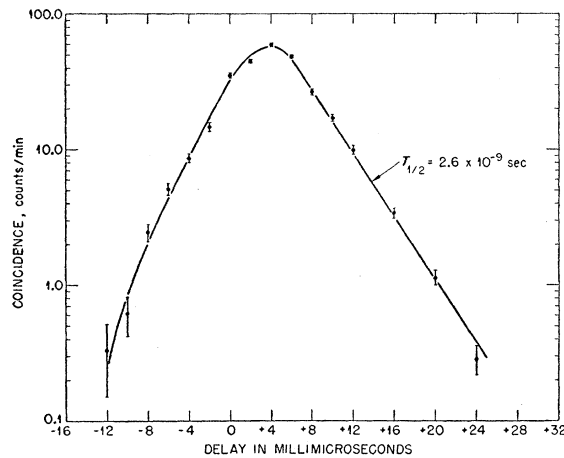


FIG. 5. Sm^{146} K x-ray- γ -ray delayed coincidence curve.

For these measurements two NaI crystals were mounted on two 14-stage 6810A RCA photomultiplier tubes which were operated at a voltage high enough so that the coincidence circuit was triggered by the first photoelectron. The half-life of the 61-keV level was found to be $2.6 \mu\text{sec}$ from the delayed coincidence curve shown in Fig. 5.

Coincidence measurements were also made with a $0.5\text{-}\mu\text{sec}$ resolving time between the low-intensity radiations shown in Fig. 2 and the K x-rays and 61-keV gamma ray. Both K x-rays and gamma rays were coincident with the continuous inner bremsstrahlung spectrum. However, only the K x-rays were in coincidence with the 485-keV gamma ray. The ratio of the single counting rates of the 485-keV gamma, N_γ , and the inner bremsstrahlung, N_{IB} , to the x-ray coincidence counting rates, $N_{x\gamma}$ and $N_{x\text{IB}}$,

$$R_5 = \frac{N_\gamma / N_{x\gamma}}{N_{\text{IB}} / N_{x\text{IB}}}, \quad (4)$$

is related to the capture ratio to the 485-keV level, ϵ_{485} ,

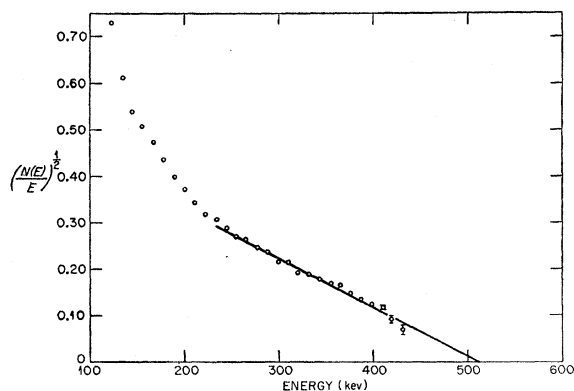


FIG. 6. Maximum energy of Sm^{146} inner bremsstrahlung spectrum.

as follows:

$$1 + \epsilon_{485} = \frac{R_5}{B_{61}[f_{K\text{cap}}'' + f_{K\text{con}}] + (1 - B_{61})f_{K\text{cap}}'''} \quad (5)$$

Here B_{61} is the fraction of electron captures that occur to the 61-keV level, $f_{K\text{cap}}''$ is the fraction of the captures to the 61-keV level that are K captures, $f_{K\text{con}}$ is the fraction of transitions from the 61-keV level that are converted in the K shell and $f_{K\text{cap}}'''$ is the fraction of the captures to the ground state that are K captures. All of the quantities in this equation, except for the capture ratio to the ground state, have been measured. This makes it possible to calculate the capture ratio to the 485-keV level if the reasonable assumption is made that the capture ratio to the ground state is approximately the same as the capture ratio to the 61-keV level. When this assumption is made, ϵ_{485} is found to be 0.61 ± 0.1 .

An estimate of the disintegration energy of Sm^{146} was obtained by analysis of the inner bremsstrahlung

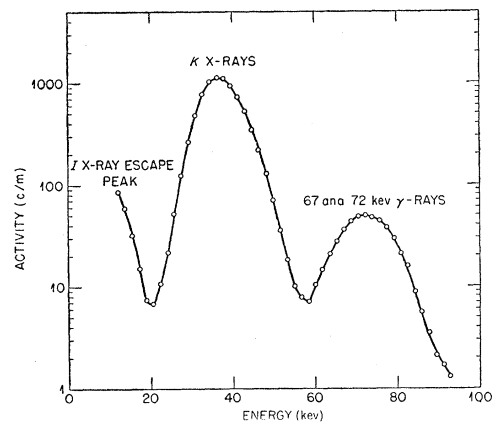


FIG. 7. Pm^{146} scintillation counter spectrum.

spectra to determine the end-point energy. Both the total spectrum and the 61-keV gamma-coincident spectrum were analyzed. The gamma spectra of Ce^{139} , Hg^{208} , Au^{198} , Sr^{86} , and Cs^{137} were used to determine the energy response and the resolution of the spectrometer and to make a somewhat arbitrary division of the spectrum at any energy into three rectangles: a peak, a Compton distribution, and a valley between these two regions. By plotting smooth curves of relative heights and widths of the three regions as a function of energy it was possible to interpolate rectangular approximations for intermediate energies.

The experimental curves were analyzed by fitting a peak rectangle to the high-energy side of the curve. The rectangular approximations to the lower energy pulses for the particular peak energy were subtracted from the original data. The remaining curve was again fitted with a new rectangular peak energy and another subtraction made. In this way a series of peak counting rates as a function of energy was obtained. These

counting rates were next corrected for detection efficiency and finally for absorption in the 585-mg/cm² tin absorber that was used to absorb the *K* x-rays and 61-keV gamma ray. These corrected values were then used to make a $[N(E)/E]^{\frac{1}{2}}$ versus *E* plot as shown in Fig. 6. The end-point energy of 540 keV obtained in this way differs from the disintegration energy by the *K* binding energy and the 61-keV level energy since most captures are to this level. The error in the 645-keV total decay energy is difficult to determine but it could be much larger than the statistical error of 3% because the $[N(E)/E]^{\frac{1}{2}}$ versus *E* plot may not be a straight line for a first forbidden transition.

PROMETHIUM-145 MEASUREMENTS

A low-geometry scintillation spectrometer gamma-ray spectrum of Pm¹⁴⁵ is shown in Fig. 7. This spectrum confirms the presence of the low-energy gamma ray previously reported by Parker and Martin.⁴ The ratio

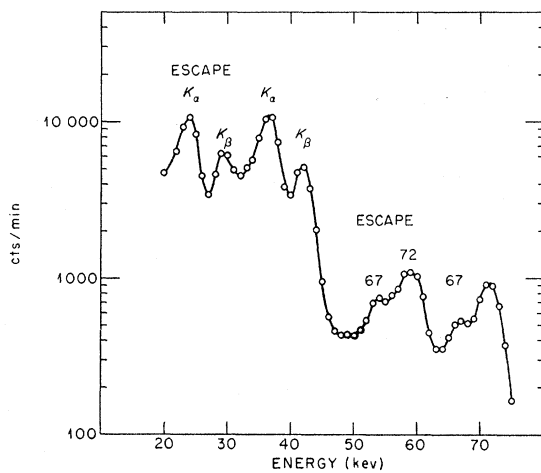


FIG. 8. Pm¹⁴⁵ proportional counter spectrum.

of *K* x-ray to gamma-ray intensity from this curve is 23.8. Spectra taken with more intense sources and tin or lead to absorb the *K* x-rays and low-energy gamma rays did not show the presence of a continuous gamma-ray spectrum. This indicates that the inner bremsstrahlung spectrum has a low-energy end point.

A Pm¹⁴⁵ spectrum taken with a krypton-filled proportional counter is shown in Fig. 8. This curve shows that the low-energy gamma radiation in the scintillation counter spectrum can be resolved into two gamma rays with energies of 67 and 72 keV. The relative intensity of these two gamma rays was the same in several different source preparations; hence both are associated with the decay of Pm¹⁴⁵. Decay of a purified Pm¹⁴⁵ source was followed with an ionization chamber for a period of two years and gave a half-life of 17.7 ± 0.4 years.

A 4π scintillation counter spectrum of the Pm¹⁴⁵ radiations which are not absorbed by 0.9-mil aluminum absorbers is shown in Fig. 9. The peaks in this spectrum

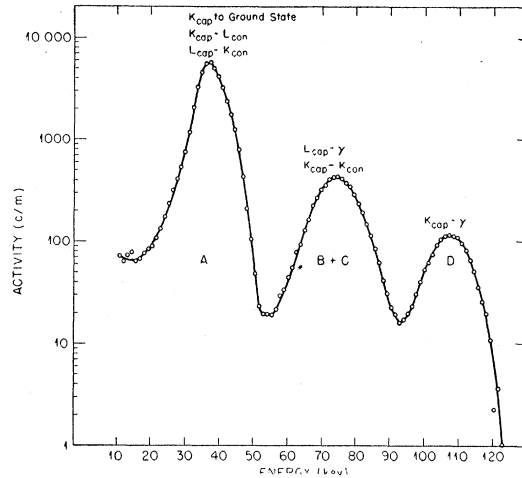


FIG. 9. 4π scintillation counter spectrum of Pm¹⁴⁵.

are labeled to conform with the labeling system used in Fig. 3. Since in this case the average gamma-ray energy is approximately double the x-ray energy, peaks *B* and *C* fall together. An independent measurement of gamma-ray intensity makes it possible to calculate the rate of the *L*_{cap-γ} process as the difference between total gammas and *K*_{cap-γ} processes. The capture ratio ϵ equal to the *L*_{cap-γ} rate divided by the *K*_{cap-γ} rate is found to be 0.93. The rate of *K* captures followed by *K* conversions can be calculated from the counting rate in the *B*+*C* peak of Fig. 9 by subtracting the number of *L*_{cap-γ} processes. It is now possible to obtain the conversion coefficient, α_K , as the ratio of *K*_{cap-Kcon} processes to *K*_{cap-γ} processes. The value of 3.33 ± 0.14 found for α_K in this way is a composite value for the 67-keV and 72-keV gamma rays.

The ratio of *K* captures to the ground state to the sum of the *K* captures to the 67- and 72-keV levels can be determined for Pm¹⁴⁵ in the same way that β was computed for Sm¹⁴⁵. In the case of Pm¹⁴⁵ the composite value of β is 5.9 ± 0.3.

Magnetic lens spectrometer measurements with a source of high specific activity and a very thin counter window are shown in Fig. 10. Because of overlapping

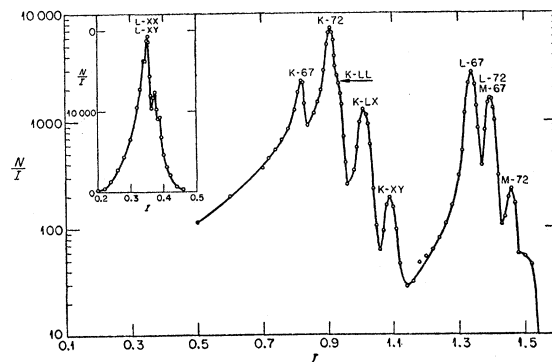


FIG. 10. Magnetic lens spectrum of Pm¹⁴⁵.

TABLE II. Pm¹⁴⁶ experimental data.

Measurement	Method	Result
<i>K/M</i> conversions 72-keV gamma ray	lens spec.	19 ± 4
<i>K/L</i> conversions 67-keV gamma ray	lens spec.	1.1 ± 0.2
$L_{67}/(L_{72}+M_{67})$ conversion electron ratio	lens spec.	1.8 ± 0.2
72-keV/67-keV <i>K</i> -conversion electrons	lens spec.	2.3 ± 0.2
<i>K</i> Auger electrons/ <i>K</i> -conversion electrons	lens spec.	0.7 ± 0.1
<i>K</i> x-rays/gamma rays	scin. spec.	23.8 ± 0.7
<i>K</i> captures to ground state/ <i>K</i> captures to excited states	4π scin. spec.	5.9 ± 0.3
<i>K</i> -conversion coeff. 67-keV gamma ray	4π scin. spec.	3.3 ± 0.3
<i>K</i> -conversion coeff. 72-keV gamma ray	4π scin. spec.	3.3 ± 0.3
72-keV gamma rays/67-keV gamma rays	delayed x-γ coinc.	2.3 ± 0.05
$(L+M+N)/K$ captures to 67-keV level	<i>L</i> -conversion electron-x-ray coinc.	0.85 ± 0.03
<i>K</i> captures/ <i>K</i> conversions	x-x and x-γ coinc.	6.56 ± 0.08
Half-life of 72-keV level	delayed x-γ coinc.	< 10 ⁻⁹ sec
Half-life of 67-keV level	delayed x-γ coinc.	3.3 × 10 ⁻⁸ sec

of the peaks shown in Fig. 10, the intensities are somewhat uncertain and values for the *K/L* conversion ratio given in Table II are therefore subject to errors other than the statistical error. From the intensities of the individual *K*-conversion peaks, the individual gamma-ray intensities in Fig. 8, and the composite α_K calculated from 4π scintillation spectrometer data it is possible to compute conversion coefficients for each of the two gamma rays. These are given in Table II.

Coincidence measurements made with a 0.5-μsec resolving time showed that x-rays were in prompt coincidence with each of the gamma rays, but that the gamma rays were not in coincidence with each other. When a proportional counter was used as the gamma-ray detector it was shown that the relative intensities of the 67- and 72-keV gamma rays were approximately the same in the *K* and *L* x-ray coincident spectra as they were in the single spectrum. This result indicates that the ratio of *K* to *L* capture to each of the levels was the same within the error of measurement which was ± 5%.

Coincidence counting rates with a 0.5-μsec resolving time were measured with scintillation counters between x-rays and gamma rays and between x-rays and x-rays. From these counting rates the ratio, R_3 , was computed as it was for Sm¹⁴⁶ and used with other constants in Eq. (3) as a check on the consistency of the various measurements.

The "fast-slow" coincidence assembly used to measure the half-life of the 61-keV level in Sm¹⁴⁶ decay was also used to study the decay of Pm¹⁴⁶. A delayed coincidence curve between the *K* x-rays and the gamma rays is shown in Fig. 11. Since the spectrum of the coincident gamma radiation shifted to smaller pulse heights as the delay was increased, it was possible to conclude that the 67-keV gamma ray was delayed more than the 72-keV gamma ray. The half-life of the 72-keV level in Nd¹⁴⁶ was too short to measure with the present equipment. The half-life of the 67-keV level was found to be 3.3 × 10⁻⁸ sec. The curve shown in Fig. 11 was used also to estimate the intensity ratio of the un-

converted 72-keV gamma to the unconverted 67-keV gamma ray given in Table II.

Because of the overlap of the *K*-conversion lines in the magnetic lens spectrum of Pm¹⁴⁶ it was not possible to use x-ray-conversion electron coincidence data in Eq. (1) to solve for the capture ratio. However, the *L*-conversion line of the 67-keV gamma ray could be resolved from other lines. The ratio of the *L*-conversion electron counting rate, N_L , to the *L*-conversion-x-ray coincidence counting rate, N_{xL} , can be used to solve for ϵ as shown in Eq. (6):

$$N_L/N_{xL} = (1 + \epsilon)/e_x \quad (6)$$

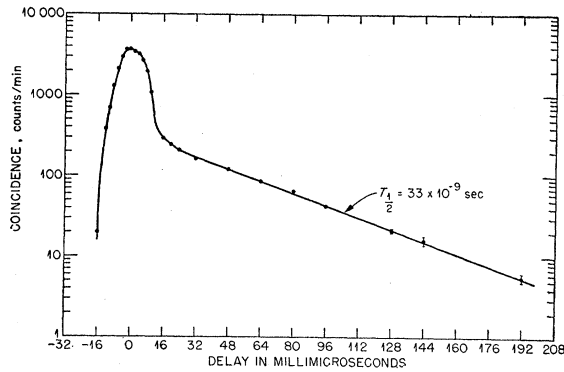
Since e_x , the x-ray counting efficiency, occurs in this equation it is necessary to know the absolute *K* x-ray emission rate and the *K* x-ray counting rate in order to solve for ϵ . A coincidence counting rate was measured between *L*-conversion electrons detected with a thin magnetic lens spectrometer and *K* x-rays counted with a scintillation spectrometer. The absolute *K* x-ray emission rate of the source was measured at low geometry with a scintillation spectrometer. The value of ϵ found for capture to the 67-keV level was 0.85 ± 0.03. In principle ϵ for capture to the 72-keV level could be determined by measuring x-ray coincidences with the *M*-conversion line. In practice the low intensity of the *M* line makes it difficult to reduce the statistical error of the measurement to the point where a difference in ϵ for capture to the two levels could be detected.

ENERGY LEVEL DIAGRAMS

The nuclear spin of the ground state of Nd¹⁴⁶ has been measured⁸ and found to be $\frac{7}{2}$. This measured spin is consistent with the shell-model prediction of $f_{1/2}$ for an 85-neutron nucleus. The shell-model prediction of $f_{7/2}$ for the ground state of Sm¹⁴⁶ should also be reliable since it has a single neutron outside a closed shell.

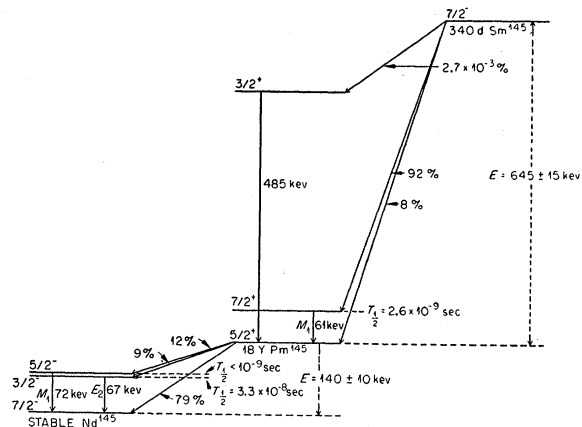
The inner-bremsstrahlung energy end point and the half-life of Sm¹⁴⁶ indicate that electron capture to either

⁸ B. Bleaney and H. E. D. Scovil, Proc. Phys. Soc. (London) A63, 1369 (1950).


 FIG. 11. Pm^{145} K x-ray-gamma-ray delayed coincidence curve.

the 61-keV level or the ground state of Pm^{145} is a first forbidden transition. The expected shell-model assignments for the lowest energy levels in a 61-proton nucleus are $\frac{7}{2}^+$ and $\frac{5}{2}^+$. With either assignment the capture transition from the $\frac{7}{2}^-$ Sm^{145} ground state would be first forbidden. Also, with either assignment electron capture to the Nd^{145} ground state in Pm^{145} decay would be first forbidden because the spin and parity changes are the same as in Sm^{145} decay. The energy computed from the L/K capture ratio to the 67-keV level in Nd^{145} and the branching ratio to this level give a comparative half-life which indicates that this transition also is first forbidden. However, the lifetimes of the 67-keV level and the K/L conversion ratio of the 67-keV gamma ray indicate that the spin change in the transition to the ground state is two. Therefore, the 67-keV level in Nd^{145} is given a $\frac{3}{2}^-$ assignment. The 72-keV level is assigned $\frac{5}{2}^-$ because the conversion coefficient of the 72-keV gamma ray indicates an M_1 transition to the ground state. The branching ratio and decay energy indicate that electron capture to the 72-keV level also is first forbidden. Since transitions from the Pm^{145} ground state to $\frac{7}{2}^-$, $\frac{5}{2}^-$, and $\frac{3}{2}^-$ levels are first forbidden with a spin change of 0 or 1, the Pm^{145} ground state must be a $\frac{5}{2}^+$ level. This argument would not be valid if the 67-keV level were fed by a 5-keV transition from the 72-keV level rather than by direct electron capture. The M -conversion electrons of such a transition were not identified in the electron energy spectrum but they could be obscured by the presence of the more intense Auger-electron spectrum in the same energy region. However, there was no evidence for an appreciable number of 5-keV transitions in the conversion-electron energy spectrum coincident with the 67-keV gamma ray where the detection sensitivity was increased several-fold.

The transitions involving the 485-keV level give some evidence in support of a $\frac{3}{2}^+$ assignment for the Pm^{145} ground state. The comparative half-life for electron capture to this level in the decay of Sm^{145} indicates that the transition is first forbidden with a spin charge of two. In capture transitions of this kind


 FIG. 12. Sm^{145} and Pm^{145} decay schemes.

the L/K ratio is high at low disintegration energies because of the relatively large amount of L III capture.⁹ The L/K capture ratios were computed from the ordinary first forbidden and the unique first forbidden transition probabilities of Brysk and Rose. In order to convert the L/K ratios to ϵ 's for comparison with experiment, the Hartree¹⁰ self-consistent field wavefunction values for Cs^+ were used to compute the relative amounts of M_1 and N_1 capture. For the experimental transition energy of 160 ± 15 keV, the computed ϵ was 0.28 ± 0.02 for an ordinary first forbidden and 0.75 ± 0.2 for a unique first forbidden transition to the 485-keV level. The experimental measurement of 0.6 ± 0.1 is in fair agreement with the computed value for the unique first forbidden case.

The most probable assignment of the 485-keV level on the basis of both capture ratio and comparative half-life is $\frac{3}{2}^+$. This assignment is also consistent with the fact that the only gamma transition from the 485-keV level observed in this work was to the $\frac{5}{2}^+$ ground state. It is estimated that if branching from the 485-keV level occurs, less than 2% of the transitions are to the 61-keV level which has been given a $\frac{7}{2}^+$ assignment.

A diagram with the Pm^{145} and Nd^{145} energy levels and the proposed spin assignments is shown in Fig. 12. The Pm^{145} disintegration energy is computed from the experimental value of ϵ for capture to the 67-keV level in Nd^{145} . The Hartree wave-function values for Cs^+ were used to convert from ϵ to an L/K capture ratio. This ratio was then used with the Brysk and Rose capture transition probabilities to compute the transition energy. The total decay energy of Pm^{145} obtained in this way is in good agreement with the value predicted from the beta-decay energy systematics of Way and Wood.¹¹

⁹ H. Brysk and M. E. Rose, Oak Ridge National Laboratory Report ORNL-1830 and errata (unpublished).

¹⁰ D. R. Hartree, Proc. Roy. Soc. (London) 143, 506 (1934).

¹¹ K. Way and M. Wood, Phys. Rev. 94, 119 (1954).

ACKNOWLEDGMENTS

We wish to thank G. W. Parker and W. J. Martin for many of the samples of Sm^{145} and Pm^{145} activity used in this work. We are indebted to W. B. Jones for arrangements in connection with the cyclotron bom-

bardment of a neodymium target. We want to thank G. E. Boyd for a sample of samarium-free neodymium which had been purified by D. H. Harris. We are particularly indebted to E. Fairstein and J. Tarrant who designed and built the fast coincidence circuit.

Neutron Thresholds in the $\text{V}^{51}(p,n)\text{Cr}^{51}$, $\text{Mn}^{55}(p,n)\text{Fe}^{55}$, $\text{Zn}^{70}(p,n)\text{Ga}^{70}$, and $\text{As}^{75}(p,n)\text{Se}^{75}$ Reactions

C. R. GOSSETT AND J. W. BUTLER

Nucleonics Division, United States Naval Research Laboratory, Washington, D. C.

(Received August 7, 1958)

The two-counter slow-to-fast ratio technique has been used with proton energies up to about 2 Mev in a study of neutron thresholds from the following four reactions. In the $\text{V}^{51}(p,n)\text{Cr}^{51}$ reaction, the ground-state threshold was measured to be 1.564 ± 0.002 Mev. No excited states were observed in the region of excitation from zero to 0.41 Mev. In the $\text{Mn}^{55}(p,n)\text{Fe}^{55}$ reaction, the ground-state threshold was measured to be 1.034 ± 0.002 Mev. Excited-state thresholds were found at 1.455 ± 0.003 and 1.982 ± 0.002 Mev, corresponding to energy levels in Fe^{55} at 0.414 ± 0.003 and 0.931 ± 0.002 Mev, respectively. In the $\text{Zn}^{70}(p,n)\text{Ga}^{70}$ reaction, the ground-state threshold was measured to be 1.457 ± 0.002 Mev. No excited states were observed in the region of excitation from zero to 0.53 Mev. In the $\text{As}^{75}(p,n)\text{Se}^{75}$ reaction, the ground-state threshold was measured to be 1.669 ± 0.002 Mev. An excited state threshold was found at 1.960 ± 0.002 Mev, corresponding to an energy level in Se^{75} at 0.287 ± 0.002 Mev. A two-counter detector of high sensitivity and a low-background experimental arrangement are described.

I. INTRODUCTION

LOW-LYING excited states of nuclides in the medium-weight region are of particular interest to the shell model. One method of observing and measuring with good precision the energies of such states is the detection of neutron thresholds from (p,n) reactions. For such reactions the thresholds of the excited states as well as the ground states may be detected by means of the two-counter slow-to-fast ratio method.¹⁻³ Furthermore, the careful measurement of the ground-state thresholds in such reactions is a precision means of measuring mass differences of neighboring isobars. Four such (p,n) reactions have been examined, and are reported herein. No excited states have been previously reported for two of the nuclides studied: Ga^{70} and Se^{75} .

A preliminary account of a part of the present experiment has been reported⁴ at a meeting of the American Physical Society.

II. EXPERIMENTAL PROCEDURE

Two of the target nuclear species, Mn^{55} and As^{75} , are monoisotopic in nature, and a third, V^{51} , has a natural abundance of 99.75%; therefore, standard laboratory cp chemicals were used in preparing these targets. The

fourth, Zn^{70} , is present in natural zinc only to the extent of 0.63%. Therefore, enriched Zn^{70} was acquired from the Stable Isotopes Division of the Oak Ridge National Laboratory, with the following isotopic abundances: Zn^{64} , 9.73%; Zn^{66} , 8.40%; Zn^{67} , 4.14%; Zn^{68} , 29.33%; and Zn^{70} , 48.40%. Targets of Mn^{55} , Zn^{70} , and As^{75} were prepared by electroplating techniques, that for Zn^{70} being basically similar to that used for nickel and cobalt in previous experiments,⁵ and those for Mn and As being the standard electroplating techniques for these elements. The vanadium target was made by the vacuum evaporation process. Target thicknesses ranged from 2 to 20 kev to the incident protons. Target backings were either gold or silver disks, $1\frac{1}{4}$ -in. diam $\times 0.010$ -in. thick.

The NRL Nucleonics Division 2-Mv Van de Graaff accelerator was used as a source of protons, providing beam currents of from 1 to 10 μa . The beam-analyzing magnet current was regulated by a proton-moment resonance device. Energy calibration was determined by means of the $\text{Al}^{27}(p,\gamma)$ resonance at 0.992 ± 0.001 Mev,^{6,7} and the $\text{Li}^7(p,n)$ threshold at 1.881 ± 0.001 Mev.^{6,8} The proton-beam energy spread was 0.06%

⁵ J. W. Butler and C. R. Gossett, *Phys. Rev.* **108**, 1473 (1957).

⁶ R. O. Bondelid and C. A. Kennedy, Naval Research Laboratory Report NRL-5083 (unpublished).

⁷ Bumiller, Staub, and Weaver, *Helv. Phys. Acta* **29**, 83 (1956); Bumiller, Staub, and Müller, *Helv. Phys. Acta* **29**, 234 (1956).

⁸ Jones, McEllistrem, Douglas, and Richards, *Phys. Rev.* **94**, 947 (1954).

¹ T. W. Bonner and C. F. Cook, *Phys. Rev.* **96**, 122 (1954).

² Brugger, Bonner, and Marion, *Phys. Rev.* **100**, 84 (1955).

³ Butler, Dunning, and Bondelid, *Phys. Rev.* **106**, 1224 (1957).

⁴ J. W. Butler and C. R. Gossett, *Bull. Am. Phys. Soc. Ser. II*, **2**, 230 (1957).